The Role of Chirality in a Set of Key Intermediates of Pharmaceutical Interest, 3-aryl-substituted-γ-butyrolactones, evidenced by Chiral HPLC Separation and by Chiroptical Spectroscopies

Daniela Rossi[1], Rita Nasti[1,§], Simona Collina,[1]*

Giuseppe Mazzeo[2,§], Simone Ghidinelli[2], Giovanna Longhi[2], Maurizio Memo[2], Sergio Abbate[2]*

[1] *Department of Drug Sciences, Medicinal Chemistry and Pharmaceutical Technology Section, University of Pavia, Viale Taramelli 12, 27100 Pavia, Italy*

[2] *Dipartimento di Medicina Molecolare e Traslazionale, Università di Brescia, Viale Europa 11, 25123 Brescia, Italy*

[§] *These two Researchers contributed equally and with primary role to the present work*

Corresponding authors at:

- Department of Drug Sciences, Medicinal Chemistry and Pharmaceutical Technology Section, University of Pavia, Viale Taramelli 12, 27100 Pavia, Italy. Tel: +39-0382987379; Fax: +39-0382422975. *E-mail address*: simona.collina@unipv.it (S. Collina)
- Dipartimento di Medicina Molecolare e Traslazionale, Università di Brescia, Viale Europa 11, 25123 Brescia, Italy. Tel: +39-0303717415; Fax: +39-0303717416. *E-mail*: *address*: sergio.abbate@unibs.it (S. Abbate)

Abstract

The enantiomers of four chiral 3-aryl-substituted-γ-butyrolactones, key intermediates for the preparation of compounds of pharmaceutical interest, were successfully isolated by enantioselective chromatography, employing the Chiralpack AD-H chiral stationary phase. For all compounds the same elution order was observed, as monitored by a full set of chiroptical methods that we employed, namely ORD (optical rotatory dispersion), ECD (electronic circular dichroism, or CD in the UV range), and VCD (vibrational circular dichroism, or CD in the IR range). By density functional theory (DFT) calculations we were able to determine that the first eluted enantiomer has (*S*) absolute configuration in all four cases. We were able to justify the elution order by molecular docking calculations for all four enantiomeric couples and suitable modeling of the stationary and mobile phases of the employed columns. The optimal performance of the chiroptical spectroscopies and of the DFT calculations allows us to formulate a lactone chirality rule out of the C=O stretching region of the VCD spectra.

Keywords: γ-butyrolactones; chiral HPLC; ORD (optical rotatory dispersion); ECD (electronic circular dichroism); VCD (vibrational circular dichroism); DFT (density functional theory); molecular docking calculations; lactone chirality rule

1. Introduction

The γ-butyrolactone ring is a five-membered cyclic scaffold widely distributed in bioactive natural products (i.e. Helenalin, Parthenolide, Fig. 1) [1], as well as in synthetic molecules of pharmaceutical interest, such as antifungal [2], anticancer [3] and antifeedant compounds [4] (Fig. 1). From a synthetic standpoint, the γ-butyrolactone can be considered a versatile key intermediate for the preparation of various compound classes, including analogues of γ-hydroxybutyric acid [5] and ω-hydroxy analogues of aminoacids [6]. Interestingly, γ-butyrolactones also represent key intermediates for the preparation of novel biologically active molecules identified in our recent researches [7,8]. Specifically, they are important intermediates for the synthesis of novel PKC ligands (Fig. 1) [7], which we recently identified within the frame of researches aimed at discovering new valuable candidates for neurodegenerative diseases treatment. Additionally, the γ-butyrolactones also represent versatile intermediates for the preparation of novel sigma 1 receptor ligands (Fig. 1) [8], which we recently identified as highly promising compounds for neuropathic pain treatment basing on our long-lasting experience in the field of sigma receptor modulators [9-18]. As clearly shown in Fig. 2, the PKC and sigma 1 receptor ligands which we had studied are both characterized by the presence of one stereogenic center and therefore are chiral. Taking into account that the enantiomers of a biologically active compound may show different interactions to the target protein and, more generally, different behavior in the biological environment, the preparation and the biological investigation of its enantiopure forms represent key steps in the drug discovery process [19,20]. Accordingly, in our ongoing research projects we are approaching the preparation of our PKC and sigma1 receptor ligands as homochiral compounds in amount and purity suitable to perform an exhaustive biological investigation. As previously discussed, the 3-aryl-substituted-γ-butyrolactones **1-3** (Fig. 2) are the key intermediates for the synthesis of both the compound classes considered. Moreover, being the first chiral intermediates of the synthetic route in both cases, they emerged as the optimal candidates for the preparation of enantiopure forms to be next used as homochiral building blocks for the asymmetric synthesis of the target compounds.

Figure 1 about here

Figure 2 about here

Herein we report on the isolation of the enantiomers of **1-3** and the assignment of their absolute configuration (AC) by a full set of chiroptical techniques (ECD = Electronic Circular Dichroism or CD in the UV range; VCD = Vibrational Circular Dichroism or CD in the IR range; ORD = Optical Rotatory Dispersion). To isolate enantiomeric **1-3**, we select enantioselective High Performance Liquid Chromatograpy (HPLC) resolution on Chiral Stationary Phases (CSPs), as a viable route for straightforward and rapid access to both the enantiomers with high optical purity and yields [13, 21-24]. Enantiomeric γ-butyrolactone **4** (Fig. 2) was also prepared and characterized as reference compound, for configurational assignment (AC) purposes [25].

In this work the employed chiroptical techniques will allow us to easily determine the AC and no contradictory indication will emerge from their use, as sometimes happens and as pointed out in the literature [26-30]. We therefore do not need to rely on the combination of the three techniques, since the answer is univocal, as recently found on Y-shaped putative drugs [31]. However we will insist somewhat more deeply on the VCD results [32], since this will allow us on the one hand to study in detail the conformational aspects of the molecules and has earned success in the assignment of the absolute configuration of natural products and drug molecules [33-38]. The latter are investigated by Density Fuctional Theory (DFT) calculations, which allow one to check also the prediction of the spectroscopic data. Finally, the AC assignment will allow us to test and to rationalize the HPLC results, about the elution order of the enantiomers. This will be studied on the basis of the DFT results and Molecular Docking “experiments”.

2. Materials and methods

2.1 Chemicals

Solvents used as eluents (HPLC grade) were obtained from Aldrich (Italy). (*R/S*)-**1-3** were prepared by us as already described [7]. The same reaction procedure was applied to the preparation of the reference compound (*R/S*)-**4** (for experimental details see supplementary information).

2.2 HPLC Separation

HPLC measurements were carried out on a Jasco system (JASCO Europe, Cremella, LC, Italy) consisting of PU-2089 plus pump, AS-2055 plus autosampler and MD-2010 plus detector. Data acquisition and control were performed using the Jasco Borwin Software.

Retention factors of first and second eluted enantiomer k_a and k_b, respectively, were calculated following IUPAC recommendations [39]; the dead time t_0 was considered to be equal to the peak of the solvent front for each particular run. Resolution was calculated according to Ph. Eur. 2.2.29 [40], enantioselectivity (α) was calculated according to: $\alpha = k_b / k_a$.

For a first rough characterization, optical rotation measurements were determined on a Jasco photoelectric polarimeter DIP 1000 (JASCO Europe, Cremella, LC, Italy) using a 0.5 dm cell and a sodium and mercury lamp (λ = 589 nm, 435 nm, 405 nm); sample concentration values (c) are given in g 10^{-2}mL^{-1}.

2.3 Chiral chromatography

In order to identify the best conditions for the resolution of (*R/S*)-**1-3** to be properly scaled up, an analytical screening was first performed using the commercially available Chiralcel OJ-H (150 mm x 4.6 mm, 5 µm), Chiralpak IC (250 mm x 4.6 mm, 5 µm), Chiralpak AD-H (150 mm x 4.6 mm, 5 µm) columns (Daicel Industries Ltd., Tokyo, Japan). The mobile phase compositions as well as the chromatographic parameters are summarized in Table SI-1 of the Supplementary Material. Sample solutions of the analyte [1 mg mL^{-1} in selected mobile phase] were filtered through 0.45 µm PTFE membranes (VWR International, Milan, Italy) before analysis. The injection volume was 10 µL, the flow rate was 1.0 mL min^{-1} and detection wavelength was 274 nm (compounds **1** and **2**) and 254 nm (compound **3**). All experiments were performed at room temperature (r.t.).

The enantiomers of (*R/S*)-**1-3** were then completely resolved by a semi-preparative process using a RegisPack column (250 mm × 10 mm, 5 µm) (Regis Technologies Inc., Morton Grove, IL, USA) according to conditions summarized in Table 1. As regards reference compound **4** , its enantiomers were resolved using the same RegisPack column (250 mm × 10

mm, 5 μm) applying the elution conditions previously described [25] with suitable modification (Table 1). The eluate was properly partitioned according to the UV profile. The collected fractions were evaporated at reduced pressure. In process control was performed using an analytical Chiralpak AD-H column.

Table 1 about here

2.4 Chiroptical Measurements

Three types of chiroptical data were considered, namely ORD, ECD and VCD. Details on instrumentation and measurement conditions are briefly described below.

a)Optical Rotatory Dispersion (ORD)

The ORD measurements were carried out with a Jasco P-2000 Polarimeter. A 10 cm micro SiO_2 cuvette was employed in all cases with $CHCl_3$ solutions at ca. 0.01 M. Solutions were studied at 25 °C and five wavelengths were considered for Optical Rotations (OR), 589 nm (Na lamp), 546, 435, 405, and 365 nm (Hg lamp). OR data were obtained with ten measurements at each wavelength and proper subtraction of the OR data from the solvent at the same wavelength was carried out. Specific rotation values were obtained from a program of the instrument. The experimental data at two adjacent wavelengths were connected through a straight line.

b)Electronic Circular Dichroism (ECD)

ECD spectra were taken from 350 to 185 nm on a Jasco 815SE spectropolarimeter. Solutions were measured in a range of ca. 0.002-0.003M/CH_3CN and were contained in 0.1 mm quartz cylindrical cuvettes. For each measurement, 10 scans were taken and averaged, considering both enantiomers of each compound **1-4**. ECD spectra of the solvent in the same experimental conditions were subtracted. Data are reported in $\Delta\varepsilon$ vs. λ (nm), from knowledge of the cell pathlength and solution concentration.

c)Vibrational Circular Dichroism (VCD)

VCD spectra were taken from 950 to 1800 nm on a Jasco FVS6000 FTIR spectropolarimeter. Solutions were ca. 0.1M/$CDCl_3$ and were contained in 200 μm BaF_2 IR cells. 5000 scans were taken for each measurement on both enantiomers of each compound **1-4**. A resolution of 4 and 8 cm^{-1} was used in recording 950-1500 cm^{-1} and 1600-2000 cm^{-1} region respectively. VCD spectra of the solvent in the same experimental conditions were obtained between the

measurements of the two enantiomers and were then subtracted and data are reported in Δε vs. ν (cm^{-1}), from knowledge of the cell pathlength and solution concentration.

2.5 DFT Calculations and Docking Simulations.

Conformational analysis of each molecule in a given configuration (*S* for **3** and **4** and *R* for **1** and **2**) was carried out at the Molecular Mechanics (MM) level, with allowance of all conformer in the range 0-5 kcal/mol from the most stable one. All these conformers were fed to Gaussian09 [41] and DFT calculated conformers and IR and VCD spectra were obtained at B3LYP/TZVP level within the PCM approximation [42]. VCD and IR spectra simulation was obtained by assigning a Lorentzian band to each calculated transition, with assigned bandwidth of 10 cm^{-1}, for the rotational and dipole strengths calculated through Gaussian09. Scaling factors of 0.96 and 0.98 were applied to the calculated VCD bands in the C=O stretching region and fingerprint region respectively. ECD and ORD calculated spectra were obtained by Gaussian09 using respectively CAM-B3LYP/TZVP and CAM-B3LYP/6-311++G(d,p) levels of theory. ECD Spectra were simulated for 0.2 wide Gaussian bands. All calculated ECD and UV absorption transitions were shifted by 10 nm and were divided by 3, to facilitate comparison with experimental data.

3. Results and discussion

Racemic **1-3** were recently synthesized within our research projects focused on the identification of new molecules potentially useful in the treatment of neurodegenerative diseases and neuropathic pain. Indeed, they are key intermediates of the synthetic pathway of both PKC [7] and sigma 1 receptor [8] ligands recently studied by us, as already stated in the introduction section (Fig. 1 and 2). More specifically, the γ-butyrolactones **1-3**, in their enantiomeric forms, represent valuable homochiral building blocks for the asymmetric synthesis of the target compounds.

Accordingly, we developed an enantioselective HPLC methodology using CSPs suitable to quickly dispose of both the enantiomers of **1-3** in g-scale with an enantiomeric purity adequate for the configurational study. To this aim, we followed the so called "fit-for purpose" strategy recently outlined at Pfizer and Vertex and applied in our recent researches for the isolation of the enantiomers of an interesting sigma 1 receptor agonist [24]. The enantiomers of reference compound **4,** whose absolute configuration had been already assigned [25], were also isolated for comparative purposes.

*3.1 Preparation of **1-4** enantiomers via enantioselective chromatography*

In the first step of our study, a primary standard screening protocol for cellulose and amylose derived CSPs [23] was applied to Chiralcel OJ-H and Chiralpak IC (cellulose derivatives) as well as to Chiralpak AD-H (amylose derivative), which are some of the most versatile CSPs available in our laboratories. Mobile phases included alcohols, such as methanol (MeOH), ethanol (EtOH) and 2-propanol (IPA), as pure solvents or in mixtures, as well as mixtures of *n*-heptane (*n*-Hep) and IPA as polar modifier. Results of the screening protocol are reported in Table SI-1 expressed in terms of retention factor (k_A or k_B), separation factor (α), and resolution factor (R_S).

Generally, poor or no separation was observed on Chiralpak IC, with the only exception of (*R/S*)-**2**, for which acceptable results were obtained only eluting with mixtures of alkane and polar modifier. As regards Chiralcel OJ-H, no separation was observed for (*R/S*)-**1** with all tested mobile phases**,** almost baseline separation was obtained for (*R/S*)-**2** eluting with mixtures of alkane and polar modifier, while good enantioseparation was achieved for (*R/S*)-**3,** eluting with mixtures of alkane and IPA, pure IPA and IPA/EtOH. Unfortunately, analysis of (*R/S*)-**3** resulted quite time-consuming and thus do not provide enough confidence for a productive scale-up.

Interestingly, results on Chiralpack AD-H turned out to be much more promising. In details, Chiralpack AD-H was the only effective CSP in the separation **1**-enantiomers, for which almost baseline separation was achieved eluting with both *n*-Hep/IPA (90/10 v/v, α = 1.06, *Rs* = 1.15) and pure MeOH (α = 1.10, *Rs* = 1.56). Good enantioselectivity and excellent resolution were obtained for both (*R/S*)-**2** and (*R/S*)-**3** eluting with n-Hep/IPA [90/10 v/v, α = 1.20, *Rs* = 3.05 for (*R/S*)-**2** and α = 1.34, *Rs* = 5.34 for (*R/S*)-**3**], within relatively short retention times. Moreover, retention behavior, enantioselectivity and resolution of **3**-enantiomers remained almost unvaried, when eluting with pure MeOH (α = 1.38, *Rs* = 5.12).

To sum up, from results of our primary screening Chiralpack AD-H clearly emerged as the optimal CSP for separating the enantiomers of (*R/S*)-**1-3** in (semi)preparative scale. Concerning the elution conditions, the best results in terms of both enantioresolution and shortest retention times were obtaining using pure MeOH for (*R/S*)-**1** and (*R/S*)-**3** and *n*-Hep/IPA (90/10 v/v) for (*R/S*)-**2** (Table SI-1). As previously discussed, none of the elution conditions experimented provided baseline separation of **1**-enantiomers. Therefore, we decided to change the polar modifier in the alkane/alcohol mobile phase, using EtOH instead of IPA. Indeed, it is well known that a change of the alcohol modifier often gives rise to a changed chiral selectivity. Accordingly, the mixture *n*-Hep/EtOH [90/10 and 85/15 (v/v)]

were experimented (Table SI-1). Unfortunately, worst results was obtained for (*R/S*)-**1**. On the contrary, the resolution of the enantiomers of both (*R/S*)-**2** and (*R/S*)-**3** was greatly improved. Particularly: *i*) good enantioselectivity and high resolution (α = 1.23, *Rs* = 3.24) combined with a slight decrease of the retention times was observed for (*R/S*)-**2** by eluting with *n*-Hep/EtOH 85/15 (v/v); and *ii*) excellent resolution of the enantiomers of (*R/S*)-**3** was observed eluting with both the mobile phase compositions (*Rs* almost 10 or higher than 10), but analysis became time-consuming, and thus not suitable for the semi preparative scale up.

To sum up, considering that shortest retention times combined with elution using a solvent as cheap as possible are important prerequisites for an economic and productive (semi)-preparative enantiomeric separation, and based on the analytical screening results (Table SI-1), we selected for the next (semi)-preparative scale-up the Chiralpack AD-H CSP, combined with pure MeOH for (*R/S*)-**1** and (*R/S*)-**3** and with *n*-Hep/EtOH 85/15 (v/v) for (*R/S*)-**2** as eluent (Fig. SI-1)

The separation of **1-3**-enantiomers in (semi)preparative scale was accomplished using a RegisPack column (250 mm × 10 mm, 5 µm) according to conditions summarized in Table 1. Actually, 22 mg of (*R/S*)-**1** were processed in 6 cycles, yielding 7.2 mg of first enantiomer (*ee* = 99.4%) and 9.2 mg of the second eluted one, along with 3.4 mg of an intermediate fraction as a mixture of the two enantiomers. Unfortunately, the analytical control of the obtained fractions revealed that the second eluted enantiomer of **1** do not meet the requisites of optical purity needed for the configurational study (ee = 78.3%). Therefore it was reprocessed under the same elution conditions, providing 7.8 mg of the target compound with the desired enantiomerical purity (*ee* = 97.7%). As regard (*R/S*)-**2,** 12 mg were processed in 3 cycles, giving 3.7 mg of the first enantiomer and 3.8 mg of the second enantiomer, both with high enantiomeric excess (*ee* ≥ 99%). Finally, 30 mg of (*R/S*)-**3** were processed in 4 cycles, yielding 10.3 mg of the first enantiomer (ee = 98.8%) and 12 mg of the second eluted one, along with 2.5 mg of an intermediate fraction as a mixture of the two enantiomers. Again, from the analytical control of the collected fractions it emerged that the second eluted enantiomer possesses low optical purity (ee = 76.8%) and thus it was processed under the same experimental conditions ultimately giving 9.5 mg of the target compound with high optical purity (ee= 98.3%). For the configurational study, the enantiomers of **4** were also isolated as reference compounds of known absolute configuration *via* enantioselective HPLC using a RegisPack column (250 mm × 10 mm, 5 µm) and applying the elution conditions previously described by Luo et al [25], with suitable modifications (Table 1). Briefly, 20 mg

of (*R/S*)-**4** were processed in two cycles yielding 8.8 mg of first enantiomer and 7.1 mg of second enantiomer with an ee higher than 95.0 %.

To sum up, by applying the recently developed "fit-for purpose" strategy, we successfully isolated the enantiomers of **1-4** *via* enantioselective HPLC in amount and enantiomeric excess suitable for configurational study, as evidenced by the chiroptical properties and process yields reported in Table 2 as well as by the final analytical control of the enantiomers collected (Fig. SI-2). It is worth noting that, as clearly stated in Table 2, using the Chiralpak AD-H (an amylose derived CSP column) the *dextro* isomers are the first eluted enantiomers for all the studied γ-butyrolactones.

Table 2 about here

3.2 Chiroptical Spectroscopies and Assignment of the Absolute Configuration

Figure 3 about here

In Fig. 3 we report the superimposed experimental VCD spectra in the C=O stretching region (1850-1700 cm^{-1}), in the so called fingerprint region (1600-950 cm^{-1}), the superimposed experimental ECD spectra and the experimental ORD traces for the two enantiomers of **4** and **3** (top part of Fig. 3) and of **1** and **2** (lower part of Fig. 3). We have decided to report the data in order of increasing molecular complexity, to better proceed in the following discussion. First of all we notice that there is an excellent mirror image aspect in the data of each couple of enantiomers. Also please notice that the color coding of the curves has always been: blue for the <u>first</u> eluted enantiomer and red for the <u>second</u> eluted enantiomer. One may also notice that the chiroptical data bear an evident correspondence with the order of elution. In particular one may observe that VCD band in the C=O stretching region and the OR data are positive for the first eluted enantiomers of all four compounds and are negative for the second eluted enantiomers (ORD data are also similar in absolute values, ranging from ca. 50 at 600 nm to 100 at 400 nm). VCD spectra of **3** and **4** are quite similar in sign and intensity for most of the VCD bands, they share with the VCD spectra of **1** and **2** just three features between 1150 and 1250 cm^{-1}, which for the first eluted enantiomer are (-,-,+) in order of increasing wavenumbers. Also ECD spectra show strong similarities in sign and shape: one may notice that the first intense band in the range of 220-230 nm is negative for the first eluted enantiomer of all molecules; for all compounds a positive band is observed between 185 and

220 nm, which though is structured differently in the four cases. While the UV spectra bear similar intensities for all four molecules (the band at ca. 200 nm has an ε of ca. 40,000), the ECD spectra of **4** and **2** are stronger than those of **1** and **3**: in the former cases the band at ca. 200 nm has Δε of ca. 10, while **3** has Δε(max)~2 and **1** has Δε(max)~4. For the proper interpretation of phenomena underlying these variations, one needs DFT calculations which will be presented below. However, even without performing calculations, one sees that the sign of most chiroptical data is in accord with the elution order, in particular the VCD band for the C=O stretchings and the ORD curves are positive for the first eluted enantiomers and negative for the second ones. Calculation will help to establish that the order of elution is related to a consistent AC, which is (*S*) for the first eluted enantiomers and (*R*) for the second ones.

In Fig. 4-left we report the comparison of DFT calculated VCD and IR spectra for the (*S*) enantiomers of **4** and **3** with the experimental VCD and IR spectra of the first eluted enantiomers of the same compounds, while in Fig. 4-right we compare DFT calculated VCD and IR spectra for the (*R*) enantiomers of **1** and **2** with the experimental VCD and IR spectra of the second eluted enantiomers of these compounds. Calculations match experiments in almost all bands, even weak ones; this allows us to conclude that the first eluted enantiomers are always (*S*), while the second eluted ones are (*R*). The best results are obtained for molecules **3** and **4**, while some minor problems are met with **1** and **2**; since also the IR spectra are predicted with a very good degree of confidence, we conclude that the conformational population is computed in an excellent way, especially for the molecules where the number of conformers is small (**3** and **4**).

Figure 4 about here

The calculated spectra are the averages through weights proportional to $e^{-(\Delta G/RT)}$; the latter weights, which are *de facto* population factors, are presented in **Table 3**, together with the values of three significant geometrical parameters and the values of the calculated rotational strength for the C=O stretching mode.

Table 3 about here

Table 4 about here

To establish how well computed VCD and ECD spectra compare with experimental ones, beyond qualitative observation, we calculated the similarity index defined in eq. 1 [43]:

$$S.I. = \frac{\int f(x)g(x)dx}{\sqrt{\int |f^2(x)|dx \int |g^2(x)|dx}} \qquad (1)$$

where *f(x)* is the computed spectrum (VCD or ECD), *g(x)* is the experimental one and *x* is the wavenumber and wavelength in the case of VCD and ECD respectively. The integral is extended to the region of interest. In the case of VCD we considered the region between 950 and 1550 cm^{-1}. The ECD data will be discussed later on. The number *S.I.* provides a performance criterion for establishing whether AC has been correctly assigned: if the number is close to +1, the assumed AC is correct; if it is close to -1 the assumed AC must be reversed. In Table 4 we report the *S.I.* values for different choices of the scaling factors and we observe that the best scaling factor is 0.98: in this case *S.I.* numbers are between 0.52-0.58 for **4**, **3** and **1**. For molecule **2** we have *S.I.* = 0.31: we noticed that this is due to the mismatch in the prediction of the negative experimental band at ca. 1000 cm^{-1} which is calculated positive. Indeed we learn from this example that the *S.I.* parameter is especially sensitive to the sign of the VCD bands and is less sensitive to their absolute values. Since qualitatively VCD spectra for **4** and **3** are excellently predicted, we conclude that a *S.I.* value of ca. +0.6 denotes unambiguous AC determination; in any case also for molecule **2** the AC is correctly determined.

The analysis of geometrical data of Table 3 allows to appreciate the relevant features of the most populated conformers of molecules **1-4** (in Figure SI-3 we provided the structure of the first two conformers). The relevant geometrical parameters are τ_1 = C(=O)CC*H, τ_2 = CC*CC, π = C(=O)CC*C. τ_1 is positive for (*S*) and negative for (*R*) and has higher absolute values (ca. 140°) for axial than for equatorial conformations (from ca. 60 to 70°); τ_2 describes the orientation of the external group; finally π describes the puckering of the lactone ring and has two values, ca. +27° for equatorial and -24° for axial conformers. One may see that, overall, the equatorial conformers dominate in population over axial conformers, being populated from 70% to 80% in the various cases. Additionally one sees that the sign of the calculated rotational strengths for the C=O stretching mode correlates with the absolute configuration, irrespective on the conformation being axial or equatorial; only its absolute value depends on conformation and is larger for axial conformers than for equatorial conformers. All these facts make the C=O stretching band a good marker of AC and finds a

nice explanation in the calculated APT (atomic polar tensor) and AAT (atomic axial tensor) for the C and O atoms in a reference axis system centered in the middle of the C=O bond, with the z-axis along C=O, y perpendicular to the lactone plane O=CCO and x lying on the latter plane (see Table SI-2): since their scalar product defines the rotational strengths [32], one may see that, due to cancellation in the other two directions, the rotational strength is generated by the y-components of the APT and AAT of the C and O atoms defining the C=O bond. The y-component of the AAT is related to a ring current in the lactone ring initiated by the C=O stretching. In SI we also provide the three-dimensional structures for the two most populated conformers of the four molecules according to Table 3. Another good marker of the lactone configuration is the (-,-,+) triplet of bands in order of increasing wavenumbers for the (*S*) enantiomer (and (+,+,-) for the (*R*) enantiomer) between 1150 and 1250 cm^{-1}; as of Figure SI-4, one sees that such bands originate from normal modes involving the C-O stretching mode of the lactone moiety.

Figure 5 about here

Also the ECD spectra and ORD curves are excellently predicted by TD-DFT calculations, as one may see from Fig. 5, where results are for the (*S*) enantiomers of **4** and **3** and for the (*R*) enantiomers of **1** and **2** respectively. In all cases signs are perfectly predicted for each ECD band as well as for the all four ORD curves; just one may observe that calculated ECD and UV absorption spectra of the four molecules are overall a bit too intense and we had to scale them down. Referring to Table 4 we may look at the *S.I.* parameter for judging the performance of calculated ECD spectra. The *S.I.* parameters are all above +0.75 and for **4** and **2** are above +0.90: this means that the assumed AC for **1-4** is correct. The high values for *S.I.* are due to the fact that ECD bands are less in number than in the VCD case; smaller *S.I.* values are found for **3** where the positive ECD band at high energy is incorrectly predicted in sign; similar reasons hold for the small *S.I.* value for **2**. The calculated ORD values instead do not show a unique trend; they are either exact or small in absolute value.

A last comment on the ECD spectra is that the single ECD bands are not assignable to C=O $n\rightarrow\pi^*$ or to $\pi\rightarrow\pi^*$ transitions in the aromatic moieties, which mutually influence each other; besides the $n\rightarrow\pi^*$ transition in lactones is quite different from ketones, as pointed out by Klyne [44-46] in the early days of CD spectroscopy, making it of limited use for configurational assignment. This provides the C=O stretching VCD data a great value for AC assignment. Indeed the latter data may acquire the significance of a configurational marker. Additionally we may state that also the (-,-,+)/(+,+,-) triplet between 1150 and 1250 cm^{-1} are

marker of the absolute configuration of the lactone ring, being associated to C-O single bond stretching and we notice that Klyne had pointed out the special character of the C-O lactone bond in association with corresponding C=O bond [45-46].

In any case from all the chiroptical data we conclude with no possible doubt that the AC is unambiguously defined: for all molecules **1-4** the first eluted enantiomer has (*S*) configuration and the second eluted enantiomer has (*R*) configuration. Such an Occam-razor conclusion is not universal for all chiral molecules [32] and especially for pharmaceutically relevant molecules [29,38] or for natural products [37,47]. It is noteworthy also that the same type of column determines the same order of elution in enantiomeric separation; this will be investigated in the next paragraph.

3.3 Docking Numerical Experiments

In the present paragraph we comment the results for the docking numerical experiments for the two enantiomers of each molecule **1**-**4** onto the stationary phase of the AD-H columns, namely amylose tris-(3,5-dimethylphenylcarbamate) polymer. The 3D-structure of the four molecules was obtained from the previous DFT analysis: we considered just the most populated conformer of Table 3. The 3D-polymer structure of amylose tris-(3,5-dimethylphenylcarbamate) in AD-H was obtained from PDB at ref. 48. AutoDock Tools (ADT) was downloaded free of charge from the web [49] and was used to prepare input file for docking simulations. The docking studies were carried out with AutoDock 4.2 (Scripps Research Institute, USA). The grid box was set to 70x70x70 (Å) with 0.375 Å spacing. Lamarckian genetic algorithm was used with 100 runs, population size of 300, maximum number of 500,000 energy evaluations, a mutation rate of 0.02 and a crossover rate of 0.50. The mobile phase was accounted for by the use of the dielectric constant corresponding to it, namely: *i*) methanol for (*R/S*)-**1** and (*R/S*)-**3**; *ii*) weighted average of *n*-heptane/ethanol (85/15, v/v) for (*R/S*)-**2**; and *iii*) weighted average of *n*-heptane/ethanol (95/5, v/v) for (*R/S*)-**4**.

The mean docking energy of (*R*) and (*S*) enantiomers are compared in Table 5. The energies are consistent with the chromatography results: longer elution times are indeed systematically associated with larger absolute values of the calculated binding energy in each one of the four enantiomeric couple.

Table 5 about here

The results are quite explicative about the systematic preference of the (*S*) configuration in being first eluted; this may be further appreciated by looking at Fig. 6 where the structure of amylose tris-(3,5-dimethylphenylcarbamate) polymer with either one of the two enantiomers of **1** is reported. One may see that the (*S*) enantiomer fits into amylose better than the (*R*) enantiomer; binding is ensured by a shorter hydrogen bonding.

Figure 6 about here

4. Conclusions

In this work we have carried out the HPLC enantiomeric separation in semi-preparative scale of four closely related chiral 3-aryl-substituted-γ-butyrolactones, which are intermediates for reactions to several pharmaceutically relevant molecules, including novel sigma 1 receptor ligands as well as novel PKC ligands. We demonstrated that the first eluted enantiomer has always (*S*) configuration. The determination of the absolute configuration has been made possible by three chiroptical spectroscopies, ECD, VCD and ORD and by DFT calculations. The three methods have given a unanimous answer to the problem of the absolute configuration assignment, which is rather an exception than a rule [30,32,38]. Finally we have been able to justify the observed constancy in elution order, through Molecular Docking numerical experiments, by evaluating free energy values of interaction of each enantiomeric couple to amylose derived chiral stationary phase of the employed columns.

Acknowledgements

We thank CINECA, via Magnanelli, Bologna, Italy for granting computer time to carry out calculations presented here. We thank CARIPLO foundation and AGROFOOD LAB at University of Brescia for financial support. We also wish to thank Dr. Silvia Meneghini, University of Pavia, Italy, for initial contribution to the present work.

REFERENCES

[1] A. Ghantous, H. Gali-Muhtasib, H. Vuorela, N.A. Saliba, N. Darwiche, What made sesquiterpene lactones reach cancer clinical trials?, Drug Discov. Today 15 (2010) 668–679.

[2] F. Jun-Tao, W. De-Long, W. Yong-Ling, Y. He, Z. Xing, New antifungal scaffold derived from a natural pharmacophore: Synthesis of a-methylene-c-butyrolactone derivatives and their antifungal activity against *Colletotrichum lagenarium*, Bioorg. Med. Chem. Lett. 23 (2013) 4393–4397.

[3] W. G1adkowski, A. Skrobiszewski, M. Mazur, M. Siepka, A. Pawlak, B. Obminska-Mrukowicz, A. Bia1onska, D. Poradowski, A. Drynda, M. Urbaniak, Synthesis and anticancer activity of novel halolactones with b-aryl substituents from simple aromatic aldehydes, Tetrahedron 69 (2013) 10414–10423.

[4] A. Skrobiszewski, W. Gladkowski, P. Walczak, A. Gliszczyn‘ Ska, G. Maciejewska, T. Klejdysz, J. Nawrot, C. Wawrzen‘ Czyk. Synthesis of *β*-aryl-*γ* -lactones and relationship: Structure – antifeedant and antifungal activity, J. Chem. Sci. 127 (2015) 687–699.

[5] J.J. Bourguignon, A. Schoenfelder, M. Schmitt, C.G. Wermuth, V. Hechler,s B. Charlier, M. Maitre. Analogues of γ-Hydroxybutyric Acid. Synthesis and Binding Studies, J. Med. Chem 31 (1988) 893–897.

[6] S. Englisch-Peters. Synthesis of ω-hydroxy analogues of valine, leucine and isoleucine Tetrahedron 45 (1989) 6127–6134.

[7] D. Rossi, V. Talman, G. Boije Af Gennas, A. Marra, P. Picconi, R. Nasti, M. Serra, J. Ann, M. Amadio, A. Pascale, R. K. Tuominen, J. Yli Kauhaloma, J. Lee, S. Collina. Beyond the affinity for protein kinase C: exploring 2-phenyl-3-hydroxypropyl pivalate analogues as C1 domain-targeting ligands, Med. Chem. Comm 6 (2015) 547-554.

[8] Università di Pavia. Use of Arylalkanolamines as Sigma-1 receptor antagonists. WO2015132733 (2015).

[9] A. Marra, D. Rossi, L. Pignataro, C. Bigogno, A. Canta, N. Oggioni, A. Malacrida, M. Corbo, G. Cavaletti, M. Peviani, D. Curti, G. Dondio, S. Collina, Toward the identification of neuroprotective agents: g-scale synthesis, pharmacokinetic evaluation and CNS distribution of (*R*)-RC-33, a promising Sigma1 receptor agonist. Future Med. Chem. 8 (2016) 287–295.

[10] M.Peviani, E. Salvaneschi, L. Bontempi, A. Petese, A. Manzo, D. Rossi, M. Salmona, S. Collina, P. Bigini, D. Curti. Neuroprotective effects of the Sigma-1 receptor (S1R) agonist PRE-084, in a mouse model of motor neuron disease not linked to SOD1 mutation, Neurobiol. Dis. 62 (2014) 218–232.

[11] S. Collina, R. Gaggeri, A. Marra, A. Bassi, S. Negrinotti, F. Negri, D. Rossi. Sigma receptor modulators: A patent review, Expert Opin. Ther. Pat. 23 (2013) 597–613.

[12] D. Rossi, A. Pedrali, A. Marra, L. Pignataro, D. Schepmann, B. Wünsch, L. Ye, K. Leuner, M. Peviani, D. Curti, O. Azzolina, S. Collina. Studies on the Enantiomers of RC-33 as Neuroprotective Agents: Isolation, Configurational Assignment, and Preliminary Biological Profile, Chirality 25 (2013) 814–822.

[13] D. Rossi, A. Pedrali, R. Gaggeri, A. Marra, L. Pignataro, E. Laurini, V. DalCol, M. Fermeglia, S. Pricl, D. Schepmann, B Wünsch, M Peviani, D. Curti, S. Collina. Chemical, pharmacological, and in vitro metabolic stability studies on enantiomerically pure RC-33 compounds: Promising neuroprotective agents acting as σ1 receptor agonists, Chem. Med. Chem. 8 (2013) 1514–1527.

[14] D. Rossi, A. Marra, P. Picconi, M. Serra, L. Catenacci, M. Sorrenti, E. Laurini, M.Fermeglia, S. Price, S. Brambilla, N. Almirante, M. Peviani, D. Curti, S. Collina,Identification of RC-33 as a potent and selective _1 receptor agonistpotentiating NGF-induced neurite outgrowth in PC12 cells. Part 2: g-scalesynthesis, physicochemical characterization and in vitro metabolic stability, Bioorg. Med. Chem. 21 (2013) 2577–2586.

[15] D. Rossi, A. Pedrali, M. Urbano, R. Gaggeri, M. Serra, L. Fernández, M. Fernández, J. Caballero, S. Ronsisvalle, O. Prezzavento, D. Schepmann, B. Wuensch, M. Peviani, D. Curti, O. Azzolina, S. Collina. Identification of a potent and selective ρ1 receptor agonist potentiating NGF-induced neurite outgrowth in PC12 cells, Bioorg. Med. Chem. 19 (2011) 6210–6224.

[16] D. Rossi, M. Urbano, A. Pedrali, M. Serra, D. Zampieri, M.G. Mamolo, C. Laggner, C. Zanette, C. Florio, D. Schepmann, B. Wuensch, O. Azzolina, S. Collina. Design, synthesis and SAR analysis of novel selective σ1 ligands (Part 2), Bioorg. Med. Chem. (2010) 18 1204–1212.

[17] D. Zampieri, M.G. Mamolo, E. Laurini, C. Zanette, C. Florio, S. Collina, D. Rossi, O. Azzolina, L. Vio. Substituted benzo[d]oxazol-2(3H)-one derivatives with preference for the σ1 binding site, E. J. Med. Chem 44 (2009) 124-130.

[18] S. Collina, G. Loddo, M. Urbano, L. Linati, A. Callegari, F. Ortuso, S. Alcaro, C. Laggner, T. Langer, O. Prezzavento, G. Ronsisvallef, O. Azzolina. Design, synthesis, and SAR analysis of novel selective σ1 ligands, Bioorg. Med. Chem. 15 (2007) 771–783.

[19] I. Agranat, H. Caner, J. Caldwell. Putting chirality to work: the strategy of chiral switches, Nat. Rev. Drug Discovery 1 (2002) 753–768.

[20] T. Andersson, Single-isomer drugs: true therapeutic advances, Clin. Pharmacokinet. 43 (2004) 279–285.

[21] Y. Okamoto, T. Ikai, Chiral HPLC for efficient resolution of enantiomers, Chem. Soc. Rev. 37 (2008) 2593–2608

[22] S. Collina, G. Loddo, M. Urbano, D. Rossi, M.G. Mamolo, D. Zampieri, S. Alcaro, A.A. Gallelli, O. Azzolina, Enantioselective Chromatography and Absolute Configuration of N,N-Dimethyl-3-(naphthalen-2-yl)-butan-1-amines: Potential Sigma1 Ligands, Chirality 18 (2006) 245–253.

[23] R. Gaggeri, D. Rossi, S. Collina, B. Mannucci, M. Baierl, M. Juza, Quick development of an analytical enantioselective high performance liquid chromatography separation and preparative scale-up for the flavonoid Naringenin, J.Chromatogr.A 1218 (2011) 5414–5422 .

[24] D. Rossi, A. Marra, M. Rui, S. Brambillab, M. Juzac, S. Collina, “Fit-for-purpose” development of analytical and (semi)preparativeenantioselective high performance liquid and supercritical fluidchromatography for the access to a novel σ_1 receptor agonist, J. Pharm. Biom. Anal. 118 (2016) 363–369

[25] Y. Luo, A.J. Carnell, Chemoenzymatic Synthesis and Application of Bicyclo[2.2.2]octadiene Ligands: Increased Efficiency in Rhodium-Catalyzed Asymmetric Conjugate Additions by Electronic Tuning, Angew Chem Int Ed 49 (2010) 2750–2754.

[26] P. Scafato, F. Caprioli, L. Pisani, D. Padula, F. Santoro, G. Mazzeo, S. Abbate, F. Lebon, G. Longhi, Combined use of three forms of chiroptical spectroscopies in the study of the absolute configuration and conformational properties of 3-phenylcyclopentanone, 3-phenylcyclohexanone, and 3-phenylcycloheptanone, Tetrahedron, 69 (2013) 10752-10762

[27] P.L. Polavarapu, Determination of the Structures of Chiral Natural Products Using Vibrational Circular Dichroism, Chapter 11 (pp. 387-420) In Comprehensive Chiroptical Spectroscopy (Applications in Stereochemical Analysis of Synthetic Compounds, Natural Products, and Biomolecules) Vol. Two, Edited by N. Berova, P.L. Plavarapu, K. Nakanishi, R.W. Woody, John Wiley & Sons, NY, 2012

[28] G. Marcin, Configurational and Conformational Study of (-)-Oseltamivir Using a Multi-Chiroptical Approach, Organic & Biomolecular Chemistry 13 (2015) 2999-3011

[29] P.L. Polavarapu, Determination of the Absolute Configurations of Chiral Drugs Using Chiroptical Spectroscopy, Molecules 21 (2016) 1056; doi:10.3390/molecules21081056

[30] P.L. Polavarapu, Why is it Important to Simultaneously Use More Than One Chiroptical Spectroscopic Method for Determining the Structures of Chiral Molecules? Chirality 20 (2008) 664–672

[31] D. Rossi, Rita Nasti, A. Marra, S. Meneghini, G. Mazzeo, G. Longhi, M. Memo, B. Cosimelli, G. Greco, E. Novellino, F. Da Settimo, C. Martini, S. Taliani, S. Abbate, S. Collina, Enantiomeric 4-Acylamino-6-alkyloxy-2 Alkylthiopyrimidines As Potential A3 Adenosine Receptor Antagonists: HPLC Chiral Resolution and Absolute Configuration Assignment by a Full Set of Chiroptical Spectroscopy, Chirality 28 (2016) 434–440

[32] L.A. Nafie, Vibrational Optical Activity-Principles and Applications, Wiley, NY, 2011

[33] S. Abbate, G. Longhi, F. Lebon, M. Tommasini, Electronic and vibrational circular dichroism spectra of (R)-(-)-apomorphine, Chemical Physics, 405 (2012) 197-206

[34] S. Abbate, L. F. Burgi, F. Gangemi, R. Gangemi, F. Lebon, G. Longhi, V. Pultz, D. A. Lightner, Comparative Analysis of IR and Vibrational Circular Dichroism Spectra for a series of Camphor related molecules, The Journal of Physical Chemistry A 113(42) (2009) 11390-11405

[35] S. Abbate, G. Longhi, E. Castiglioni, F. Lebon, P.M. Wood, Lawrence W. L. Woo, Barry V. L. Potter, Determination of the Absolute Configuration of Aromatase and Dual Aromatase-Sulfatase Inhibitors by Vibrational and Electronic Circular Dichroism Spectra Analysis, Chirality, 21 (2009) 802-809

[36] P.M Wood, L.W. Lawrence Woo, J.R. Labrosse, M.N. Trusselle, S. Abbate, G. Longhi, E. Castiglioni, F. Lebon, A. Purohit, M.J. Reed, B.V. L. Potter, Chiral Aromatase and Dual

Aromatase-Steroid Sulfatase Inhibitors from the Letrozole Template: Synthesis, Absolute Configuration, and In Vitro Activity, Journal of Medicinal Chemistry 51 (2008) 4226–4238

[37] S. Abbate, L.F. Burgi, E. Castiglioni, F. Lebon, G. Longhi, E. Toscano, S. Caccamese, Assessment of configurational and conformational properties of Naringenin by Vibrational Circular Dichroism, Chirality 21 (2009) 436-441

[38] Y.He, W.Bo, R.K. Dukor, L.A. Nafie, Determination of absolute configuration of chiral molecules using vibrational optical activity: a review, Applied Spectroscopy 65 (2011) 699-723

[39] L.S. Ettore, Nomenclature for Chromatography**,** Pure Appl. Chem. 65 (1993) 819–872.

[40] European Pharmacopoeia, 2.2.29. LIQUID CHROMATOGRAPHY, 8th ed., EDQM,European Pharmacopoeia, Council of Europe, B.P. 907, 67029 Strasbourg,France, July 2013.

[41] Gaussian 09, Revision A.02, Frisch MJ, Trucks GW, Schlegel HB, Scuseria GE, Robb MA, Cheeseman JR, Scalmani G, Barone V, Mennucci B, Petersson GA, Nakatsuji H, Caricato M, X L, Hratchian HP, Izmaylov AF, Bloino J, Zheng G, Sonnenberg JL, Hada M, Ehara M, Toyota K, Fukuda R, Hasegawa J, Ishida M, Nakajima T, Honda Y, Kitao O, Nakai H, Vreven T, Montgomery JA Jr, Peralta JE, Ogliaro F, Bearpark M, Heyd JJ, Brothers E, Kudin KN, Staroverov VN, Kobayashi R, Normand J, Raghavachari K, Rendell A, Burant JC, Iyengar SS, Tomasi J, Cossi M, Rega N, Millam JM, Klene M, Knox JE, Cross JB, Bakken V, Adamo C, Jaramillo J, Gomperts R, Stratmann RE, Yazyev O, Austin AJ, Cammi R, Pomelli C, Ochterski JW, Martin RL, Morokuma K, Zakrzewski VG, Voth G, Salvador P, Dannenberg S, Dapprich S, Daniels AD, Farkas Ö, Foresman JB, Ortiz JV, Cioslowski J, Fox DJ. Gaussian. Gaussian, Inc.: Wallingford CT; 2009.

[42] J. Tomasi, B. Mennucci, R. Cammi, Quantum mechanical continuum solvation models. Chem Rev. 105 (2005) 2999-3093

[43] P.L. Polavarapu, Chiroptical Spectroscopy Fundamentals and Applications (2017) CRC Press, Taylor & Francis Group, Boca Raton, FL page 180

[44] J.P. Jennings, W. Klyne, P.M. Scopes, Optical Rotatory Dispersion. Part XXIV. Lactones, J. Chem. Soc. (1965) 7211-7229.

[45] J.P. Jennings, W. Klyne, P.M. Scopes, Optical rotatory dispersion. Part XXVI. Some bridged ring lactones, J. Chem. Soc. (1965) 7229-7237

[46] W. Klyne, P.M. Scopes, A. Williams, Optical rotatory dispersion. Part XXVII. The Hudson sector rule, J. Chem. Soc. (1965) 7237-7242

[47] G. Mazzeo, E. Santoro, A. Andolfi, A. Cimmino, P. Troselj, A.G. Petrovic, S. Superchi, A. Evidente, N. Berova, Absolute Configurations of Fungal and Plant Metabolites by Chiroptical Methods. ORD, ECD, and VCD Studies on Phyllostin, Scytolide, and Oxysporone J. Nat. Prod. 76 (2013) 588-599

[48] Y.K. Ye, S. Bai, S. Vyas, M.J. Wirth, NMR and Computational Studies of Chiral Discrimination by Amylose Tris(3,5-dimethylphenylcarbamate), J. Phys. Chem. B (2007) 1189-1198

[49] G.M. Morris, R. Huey, W. Lindstrom, M.F. Sanner, R.K. Belew, D.S. Goodsell, A.J. Olson, J. Computational Chemistry 16 (2009) 2785-91

CAPTION TO FIGURES

Figure 1. Involvement of the γ-butyrolactone ring in biologically active molecules.

Figure 2. Synthetic pathway of PKC and sigma 1 receptor ligands.

Figure 3. Superimposed VCD spectra in the C=O stretching region (first column from left), in the fingerprint region (second column), ECD spectra (third column) and ORD curves fort he two enantiomers of molecules **4** (top row), **3** (second row from top), **1** (third row) and **2** (bottom row). The first eluted enantiomer is color-coded blue in all graphs, and the second eluted one is color-coded red in all graphs.

Figure 4. Comparison of experimental (color, solid lines) with calculated (black, dashed lines) VCD spectra of molecules **4** and **3** (left columns, top and lower respectively) and of molecules **1** and **2** (right columns, top and lower respectively). Calculated spectra are Boltzmann averages from calculated spectra of each single conformer (see Table 3). Color coding as in Figure 3.

Figure 5. Comparison of experimental (color, solid lines) with calculated (black, solid lines) ECD spectra and ORD curves of molecules **4** and **3** (first left two columns) and of molecules **1** and **2** (right columns, top and lower respectively). Calculated spectra are Boltzmann averages from calculated spectra of each single conformer (see Table 3). Color coding as in Figure 4. (For molecule **3**, the Gaussian width of bands is assumed to be 0.3 eV, for the other molecules it is 0.2 eV-see Experimental Section).

Figure 6. Molecular docking analysis for compound **1** in the two enantiomeric forms *R* (left) and *S* (right) onto polymeric forms of *Amylose tris-(3,5-dimethylphenylcarbamate)* – Chiralpack® AD-H. For the structure of the molecule **1**, we used the one of the most populated conformed derived by DFT calculations (see Table 3). For the structure of the stationary phase we referred to the PDB file presented in Ref. 48.

CAPTIONS TO TABLES

Table 1. (Semi)-preparative resolution of (*R/S*)-**1-4** on a RegisPack column (250 mm × 10 mm, 5 μm).

Table 2. Chiroptical properties and isolated amounts of 1-4 enantiomers.

Table 3. Main characteristics of the most significant populated calculated conformers of molecules **1-4**: **3** and **4** in the (*S*) configuration, and **1** and **2** in the (*R*) configuration. Dihedral angles' values τ_1(°), τ_2(°) (see text for definition), calculated rotational strength for the C=O stretching mode (10^{-44} esu^2cm^2) and Boltzmann statistical weight.

Table 4. Dissymmetry factor (calculated as reported in eq. 1) of similarity between experimental and calculated VCD and ECD spectra. In brackets is reported the used scaling factors for VCD and the applied red shift in nanometer for ECD which maximize dissymmetry factor.

Table 5. Measured elution times and calculated binding energies for the two enantiomers of the four compounds studied in the presents work.

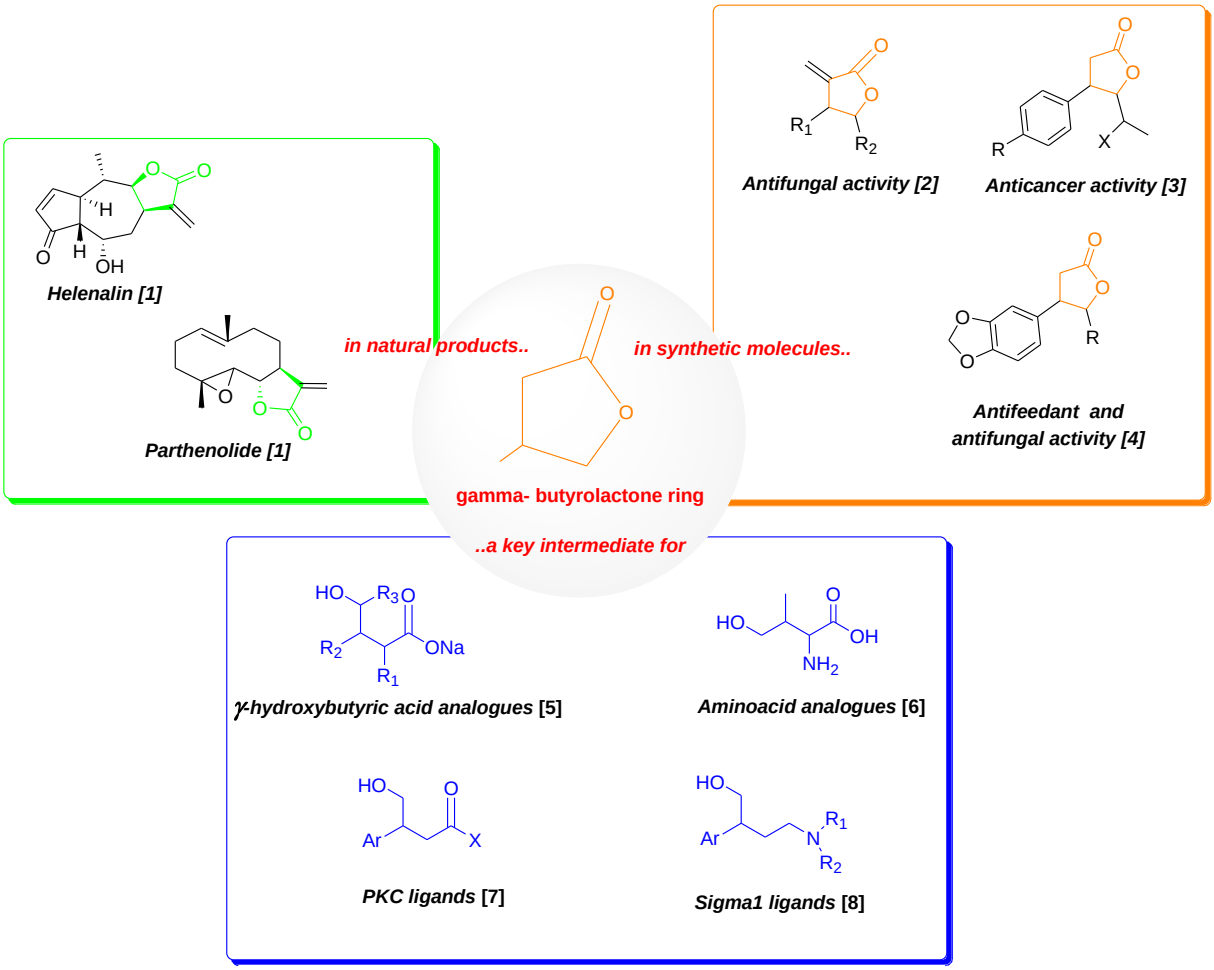

Figure 1. Involvement of the γ-butyrolactone ring in biologically active molecules.

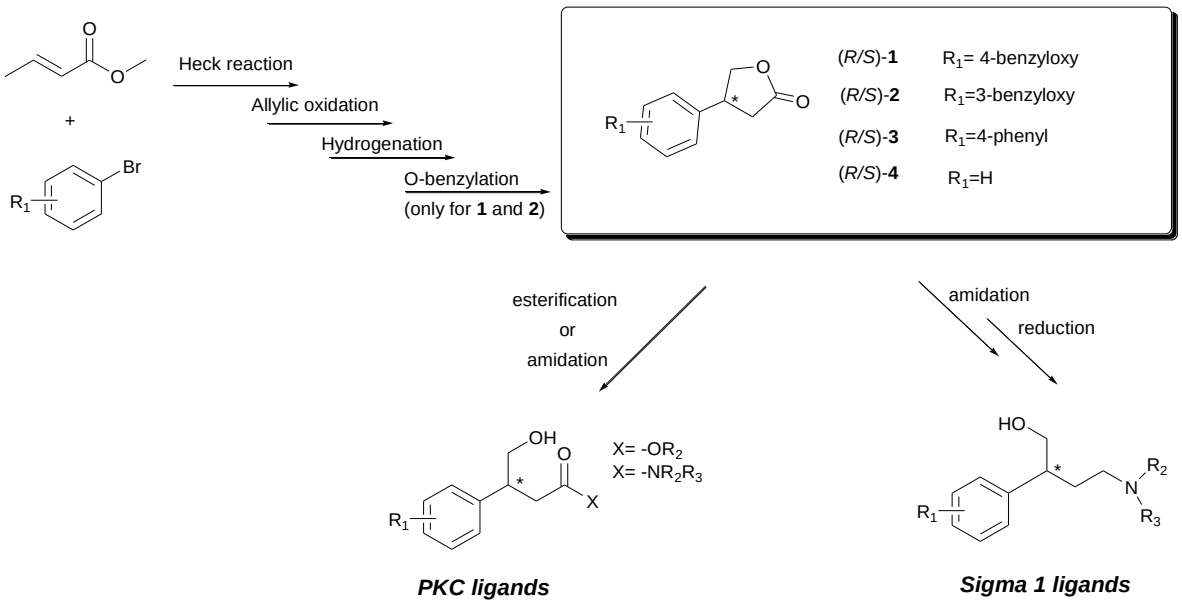

Figure 2. Synthetic pathway of PKC and sigma 1 receptor ligands.

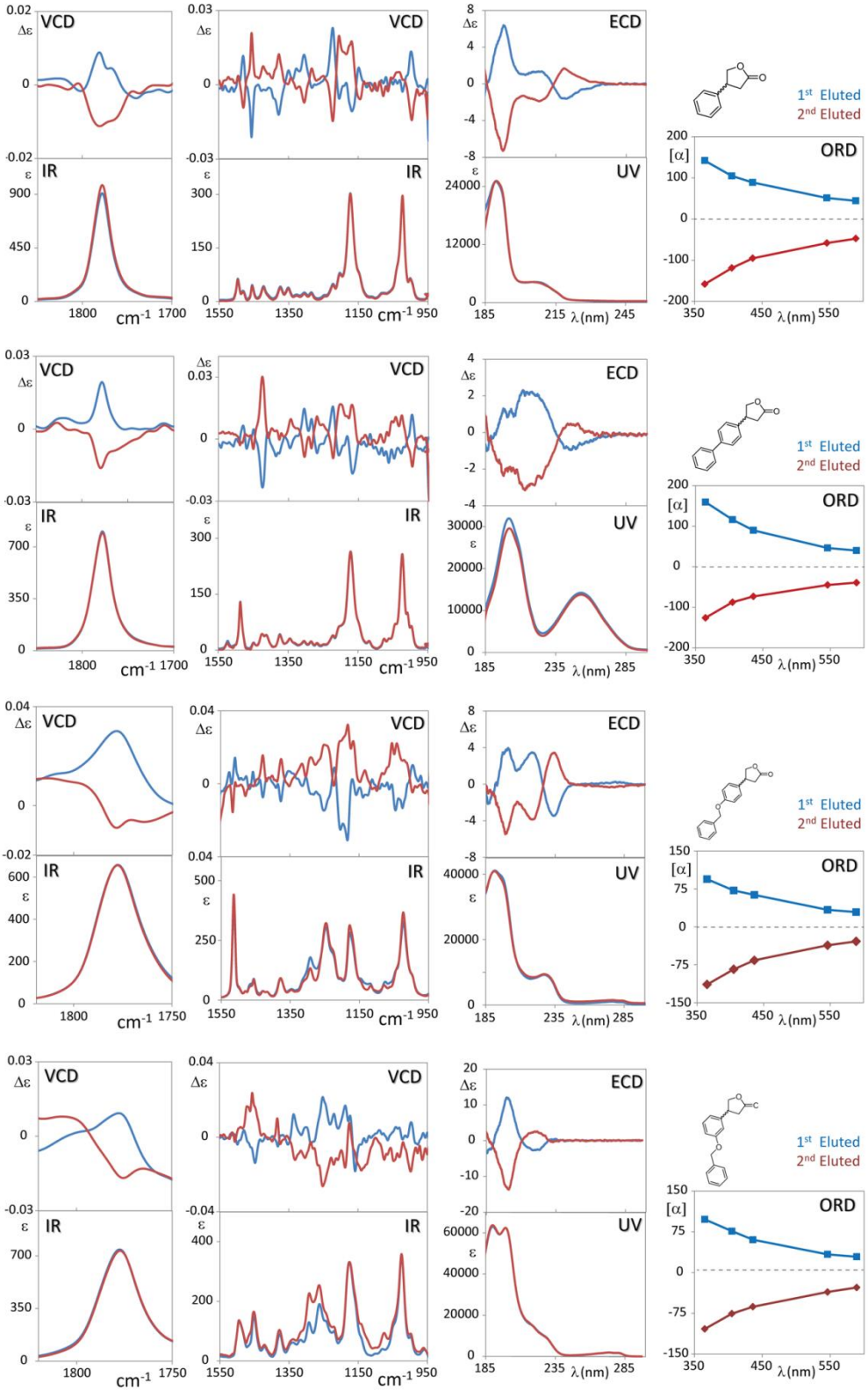

Figure 3. Superimposed VCD spectra in the C=O stretching region (first column from left), in the fingerprint region (second column), ECD spectra (third column) and ORD curves fort he two enantiomers of molecules **4** (top row), **3** (second row from top), **1** (third row) and **2** (bottom row). The first eluted enantiomer is color-coded blue in all graphs, and the second eluted one is color-coded red in all graphs.

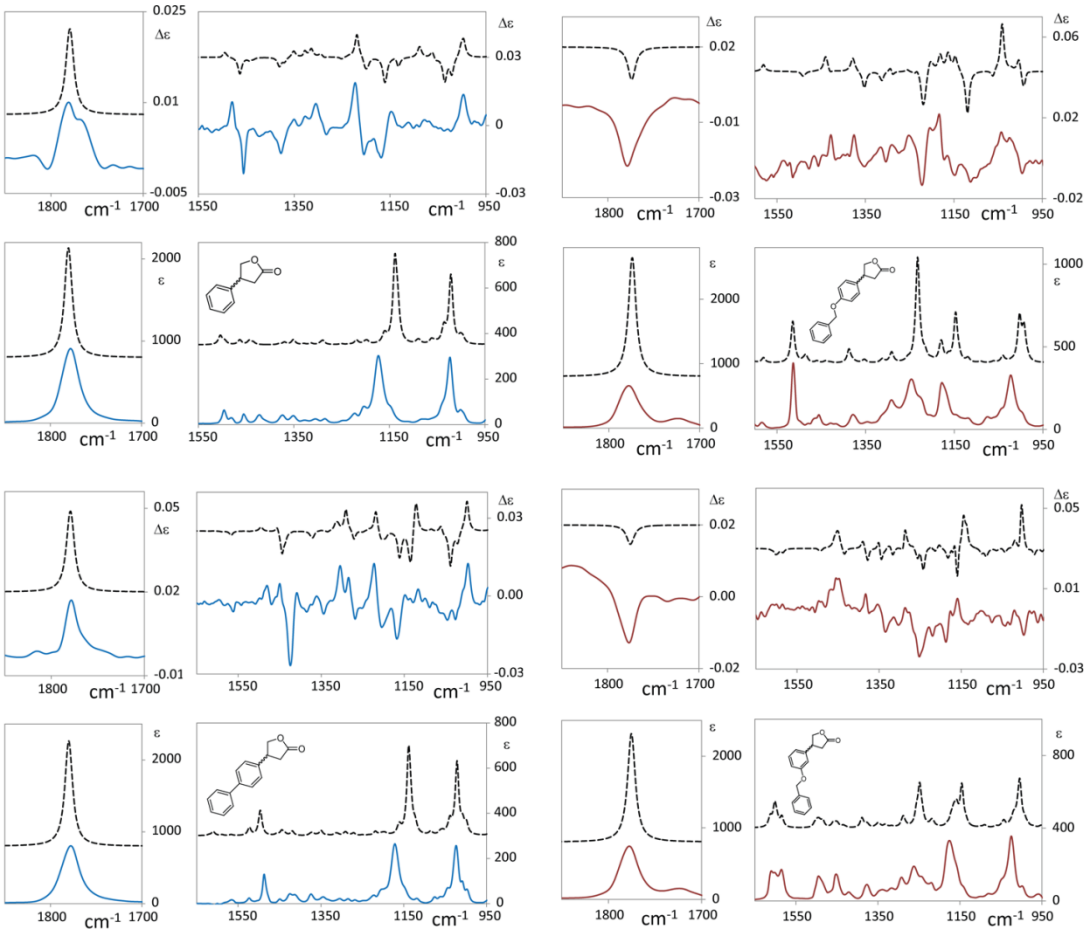

Figure 4. Comparison of experimental (color, solid lines) with calculated (black, dashed lines) VCD spectra of molecules **4** and **3** (left columns, top and lower respectively) and of molecules **1** and **2** (right columns, top and lower respectively). Calculated spectra are Boltzmann averages from calculated spectra of each single conformer (see Table 3). Color coding as in Figure 4.

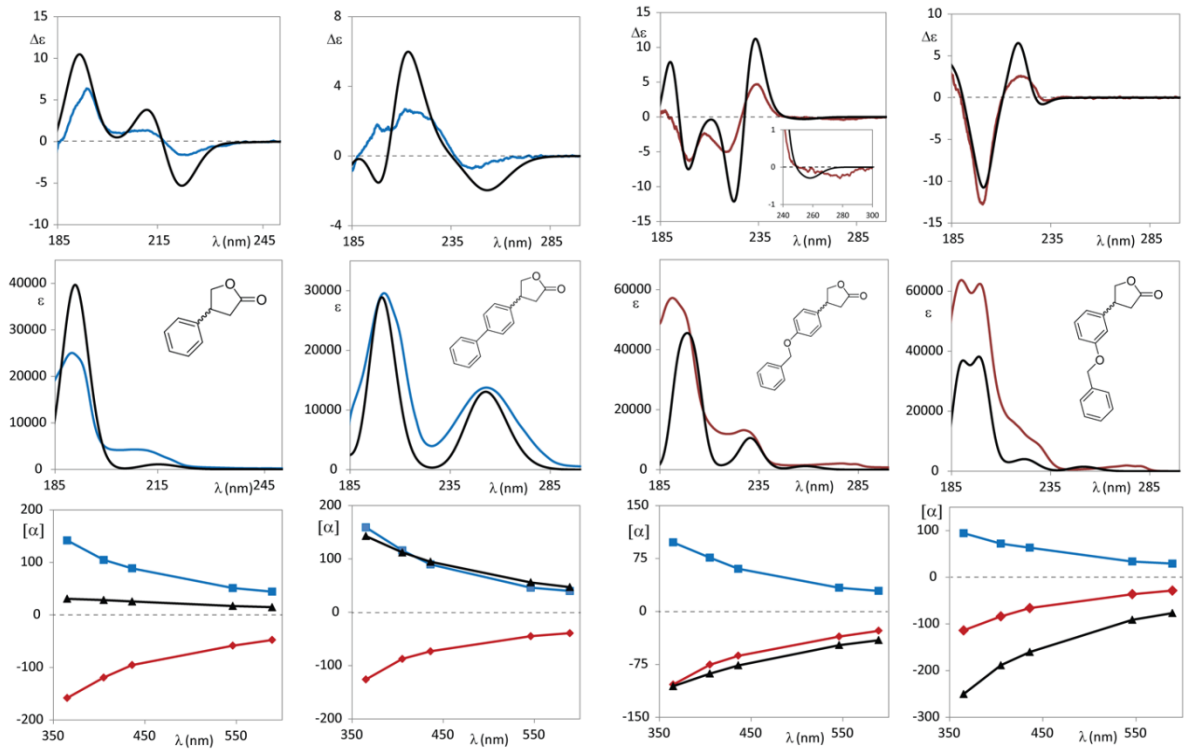

Figure 5. Comparison of experimental (color, solid lines) with calculated (black, solid lines) ECD spectra and ORD curves of molecules **4** and **3** (first left two columns) and of molecules **1** and **2** (right columns, top and lower respectively). Calculated spectra are Boltzmann averages from calculated spectra of each single conformer (see Table 3). Color coding as in Figure 4. (For molecule **3**, the Gaussian width of bands is assumed to be 0.3 eV, for the other molecules it is 0.2 eV-see Experimental Section)

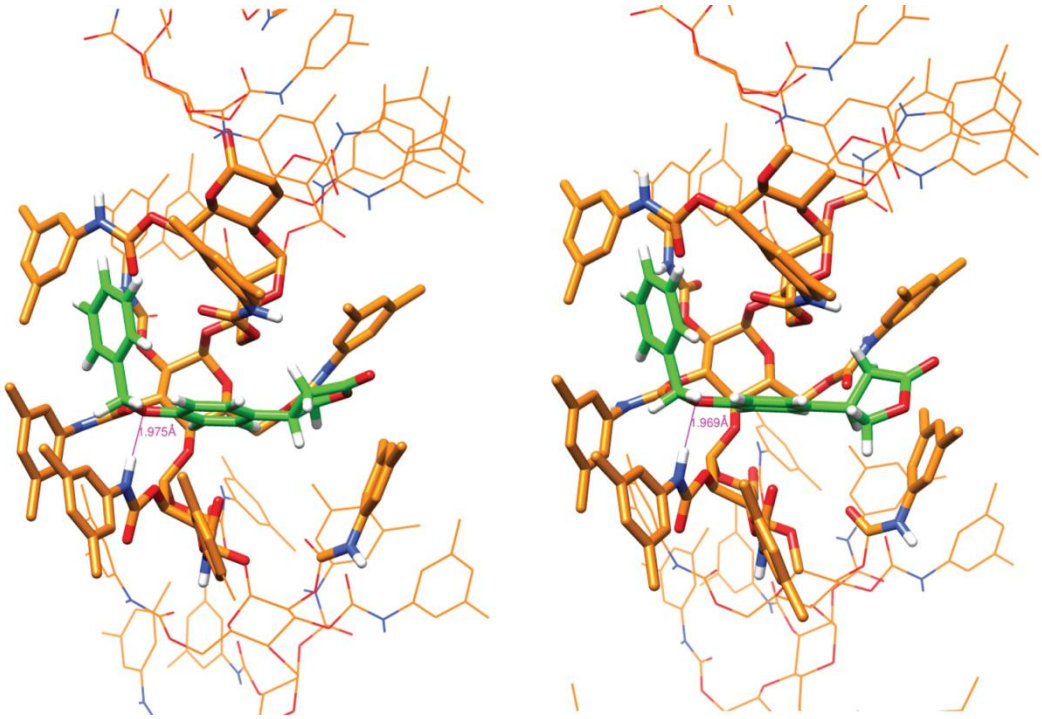

Figure 6. Molecular docking analysis for compound **1** in the two enantiomeric forms *R* (left) and *S* (right) onto polymeric forms of *amylose tris-(3,5-dimethylphenylcarbamate)* – Chiralpack® AD-H. For the structure of the molecule **1**, we used the one of the most populated conformed derived by DFT calculations (see Table 3). For the structure of the stationary phase we referred to the PDB file presented in Ref. 48.

Table 1

(Semi)-preparative resolution of (*R/S*)-**1-4** on a RegisPack column (250 mm × 10 mm, 5 µm).

Cmpd	**Mobile Phase (v/v)**	**Flow rate (mL min^{-1})**	**Tr_A (min)**	**Tr_B (min)**	**Injection volume (mL)**	**Concentration (mg mL^{-1})**
1	MeOH	4	11.63	12.44	1	4
2	*n*-Hep/EtOH 85/15	4	20.75	24.02	1	4
3	MeOH	4	16.48	21.29	2.5	3
4	*n*-Hep/EtOH 95/5	4	25.28	30.13	5	2

Table 2

Chiroptical properties and isolated amounts of **1-4** enantiomers.

Cmpd	t_R (min)	$[\alpha]_D^{20}$ [a]	Ee [%]	Isolated amount (mg)	Yield [%]
(+)-1	7.84	29.2	99.4	7.2	32.7
(-)-1	8.39	-27.42	97.7	7.8	35.4
(+)-2	13.12	29.2	99.1	3.7	31.5
(-)-2	15.51	-28.6	99.3	3.8	32.2
(+)-3	11.84	33.8	98.8	10.3	34.5
(-)-3	15.27	-33.3	98.3	9.5	31.6
(+)-4	14.04	47.4	99.9	8.8	43.7
(-)-4	16.56	-45.6	95.1	7.1	35.3

[a] c : 0.2% in $CHCl_3$

Table 3

Main characteristics of the most significant populated calculated conformers of molecules **1-4**: **3** and **4** in the (*S*) configuration, and **1** and **2** in the (*R*) configuration. Dihedral angles' values τ_1(°), τ_2(°) (see text for definition), calculated rotational strength for the C=O stretching mode (10^{-44} esu^2cm^2) and Boltzmann statistical weight.

Compound-4	τ_1	τ_2	**R**	**%pop**	π
4a	139.6	-111.2	60.9	25.6	23.9
4b	84.8	-124.3	17.5	74.4	-27.8
Compound-3	τ_1	τ_2	**R**	**%pop**	π
3a	85.4	-124.4	26.4	37.3	-27.4
3b	85.2	-123.8	29.8	32.9	-27.6
3c	138.5	-111.9	77.5	17.6	23
3d	139.5	-107.8	75.1	12.3	24
Compound-1	τ_1	τ_2	**R**	**%pop**	π
1a	-85.1	-55.5	-20.2	33.0	27.6
1b	-85.2	-56	-19.6	29.4	27.6
1c	-85.2	-57.7	-20.2	19.5	27.5
1d	-139.2	-69.4	-60	5.7	-23.9
1e	-140.2	-72.5	-59.7	3.9	-24.9
Compound-2	τ_1	τ_2	**R**	**%pop**	π
2a	-85.3	-56.4	-20.8	17.7	27.5
2b	-85.1	122.2	-1.2	17.4	27.7
2c	-84.8	-56.6	-30.4	15.6	28
2d	-58.5	123.8	6.2	11.9	27.5
2e	-139.5	-69.3	-33	7.1	-24
2f	-84.9	120.8	3.3	3.8	27.9
2g	-139.4	106.3	-27.3	3.1	-23.8
2h	-85.1	-57.2	-24.7	3.0	27.7
2i	-139.1	-74.6	-50	2.6	-23.6
2j	-139.4	105.4	-36.2	2.4	-24
2k	-83.2	17.1	5	2.1	29.2
2l	-85.2	122.7	11.7	2.1	27.6
2m	-85.5	124.2	-16.9	1.9	27.5

Table 4

Dissymmetry factor (calculated as reported in eq. x) of similarity between experimental and calculated VCD and ECD spectra. In brackets is reported the used scaling factors for VCD and the applied red shift in nanometer for ECD which maximize dissymmetry factor.

COMPOUND	**ENANTIOMER**	**VCD (0.985)**	**VCD (0.98)**	**VCD (0.975)**	**VCD (0.97)**	**ECD (Shift nm)**
4	**S**	0.56	0.58	0.46	0.25	0.92 (10)
3	**S**	0.5	0.55	0.52	0.38	0.79 (5)
1	**R**	0.49	0.52	0.37	0.23	0.77 (15)
2	**R**	0.13	0.11	0.07	0.04	0.94 (10)

Table 5

Measured elution times and calculated binding energies for the two enantiomers of the four compounds studied in the presents work.

Compound	Elution Times (min)	Mean Binding Energy (kcal/mol)
(*R*)-**1**	8.39	-7.58
(*S*)-**1**	7.84	-7.42
(*R*)-**2**	15.51	-7.70
(*S*)-**2**	13.12	-7.56
(*R*)-**3**	15.27	-8.19
(*S*)-**3**	11.84	-7.91
(*R*)-**4**	16.56	-5.93
(*S*)-**4**	14.04	-5.80